12 Detection of Focal Liver Lesions

Emilio Quaia, Maja Ukmar, and Maria Cova

CONTENTS

12.1 Detection of Liver Metastases

12.1.1 Introduction

The liver is one of the most common sites for metastatic spread of most malignancies, and the accurate assessment of liver metastatic disease is important for the planning of surgical, interventional, and medical therapy. Baseline gray-scale ultrasound (US) is routinely used as the first imaging technique in the detection of liver metastases, even though its accuracy is related to operator experience. Moreover, the general sensitivity of baseline US in the detection of liver metastases ranges between 53% and 84% (Cosgrove and Bolondi 1993; Carter et al. 1996), while US sensitivity for metastatic lesions smaller than 1 cm has been found to be as low as 20% (Wernecke et al. 1991). Most metastatic lesions missed on baseline US are either smaller than 1 cm or isoechoic relative to adjacent liver parenchyma.

The best available reference standards for imaging diagnosis of liver metastases are computed tomography (CT) and magnetic resonance (MR) imaging with agents targeted to Kupffer cells [superparamagnetic iron oxide (SPIO)] or hepatocytes [gadobenate dimeglumine (Gd-BOPTA)] (del Frate et al. 2002), CT arterial portography, and surgical exploration with intraoperative US (Robinson 2001). SPIO-enhanced MR imaging shows a higher sensitivity than iodinated contrast material-enhanced CT (99% vs 94%; Ward et al. 1999) in the detection of metastatic lesions larger than 1 cm, but its sensitivity has been reported to be much lower in lesions smaller than 1 cm (Bellin et al. 1994; Haspigel et al. 1995; Ward et al. 1999, 2000a, 2003). del Frate et al. (2002) found the sensitivity of SPIO-enhanced MR imaging to be superior to that of Gd-BOPTA-enhanced MR imaging for the detection of liver metastases. CT arterial portography is more sensitive than iodinated contrast-enhanced CT and SPIO-enhanced MR imaging in detecting metastases smaller than 1 cm, but it is an invasive imaging technique and produces more false positive lesions (Soyer et al. 1992; Seneterre et al. 1996; Valls et al. 1998). Like CT arterial portography, intraoperative US has been shown to be very sensitive but not specific in the detection of liver metastases (Robinson 2001).

Dedicated US contrast-specific techniques have shown good accuracy in the detection of liver metastases after microbubble injection (Dalla Palma et al. 1999; Harvey et al. 2000a,b; Albrecht et al. 2001a, 2003a,b; del Frate et al. 2003; Quaia et al. 2003). The first such agents to be employed for this purpose were air-filled microbubbles, such as Levovist and Sonavist (Schering AG, Berlin, Germany). After blood pool clearance, air-filled microbubbles were shown to have a late liver-specific parenchymal phase from 3 to 5 min after injection. During this time microbubbles are stationary in liver and are probably pooling in sinusoids or phagocytosed by Kupffer cells of the reticuloendothelial system (Hauff et al. 1997; Blomley et al. 1998; Bauer et al. 1999; Forsberg et al. 1999, 2000a,b, 2002; Quaia et al. 2002a). The highest microbubble detectability was achieved when the acoustic power of the US beam was high enough (mechanical index = 1.0–1.2) to destroy microbubbles, producing a transient high-

E. Quaia, MD, Assistant Professor of Radiology;
M. Ukmar, MD; M. Cova, MD, Professor of Radiology
Department of Radiology, Cattinara Hospital, University of Trieste, Strada di Fiume 447, 34149 Trieste, Italy

intensity wideband frequency signal (Dalla Palma et al. 1999a; Quaia et al. 2003). During the late phase the normal liver parenchyma displays clear uptake of air-filled microbubbles, while metastatic lesions, which are devoid of liver sinusoids and Kupffer cells, appear as hypoechoic and hypovascular defects compared to the adjacent liver.

New generation sulfur hexafluoride-filled microbubbles (Albrecht et al. 2003b) without proven liver-specific properties (Lim et al. 2004), such as SonoVue (Bracco, Milan, Italy), or perfluorocarbon-filled microbubbles with proven liver-specific properties, such as Sonazoid (Amersham Health, Oslo, Norway) (Needlman et al. 1998; Albrecht et al. 2001b; Forsberg et al. 2002b; Lesavre et al. 2003; Kindberg et al. 2003; Watanabe et al. 2003), have shown promise for the detection of liver metastases. In particular, the liver specificity of Sonazoid is similar to that of Levovist, but it shows stronger and more prolonged liver enhancement, which has obvious advantages in terms of both longer scanning opportunity and performance of US-guided biopsy of detected lesions (Albrecht et al. 2003a).

12.1.2 Scanning Modes

a) High acoustic power mode. High acoustic power insonation was the first mode employed to detect liver metastases after microbubble-based agent injection.

Dedicated contrast-specific US techniques are employed from 3 to 5 min after the injection of air-filled microbubbles during the liver-specific late phase (Blomley et al. 1998, 1999; Dalla Palma et al. 1999; Hope Simpson et al. 1999; Harvey et al. 2000a,b; Albrecht et al. 2001a,b, 2003a,b; del Frate et al. 2003; Lesavre et al. 2003; Quaia et al. 2003). The aim of high acoustic power insonation is to cause extensive microbubble rupture throughout the liver parenchyma, with production of a wideband frequency signal. Because of the transience of contrast enhancement due to microbubble destruction (Albrecht et al. 2000), the scanning technique has to be optimized to image fresh, undestroyed microbubbles with each new frame (Albrecht et al. 2003a). Moreover, since the whole liver parenchyma has to be assessed when investigating the possible presence of liver metastases, the insonation has to be continuous instead of intermittent, as in the characterization of focal liver lesions. For these reasons it is appropriate to transmit the maximal acoustic power (mechanical index >1), switching off the signal persistence and employing the lowest possible frame rate (8–10 Hz) and a single focal zone positioned in the deep third of the field of view (8–10 cm from abdominal surface) in order to minimize and to render more homogeneous the rupture of microbubbles.

Scanning is started from 3 to 5 min after microbubble bolus injection by using a dedicated contrast-specific mode (e.g., Pulse Inversion Mode from Philips-ATL, WA, USA or Agent Detection Imaging from Siemens-Acuson, CA, USA). Scanning of the liver parenchyma is performed, during breath-hold, by one or two transverse sweeps throughout the right liver lobe, and with one longitudinal sweep on the left lobe (Fig. 12.1). Microbubble rupture may produce heterogeneous contrast enhancement in the case of irregular free-hand scanning, with evidence of artifacts which may simulate focal liver lesions. After the sweeps have been completed, each stored digital cine-clip has to be reviewed to detect liver metastases appearing as hypovascular focal liver lesions against the background of enhancing normal liver parenchyma.

b) Low acoustic power mode. The low acoustic power insonation mode is employed with new-generation microbubble-based agents. Since microbubble rupture is minimized with low acoustic power insonation, the liver parenchyma may be scanned

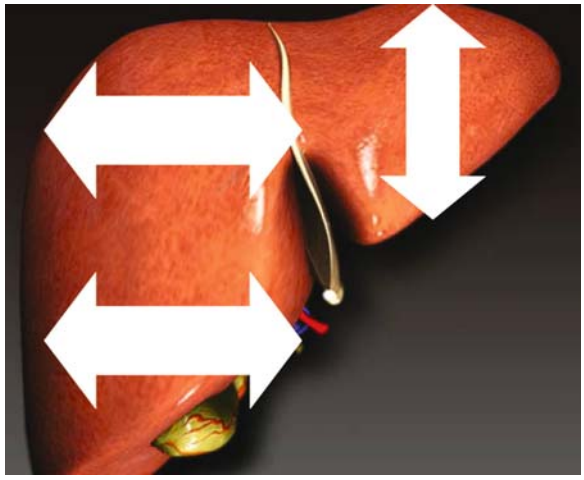

Fig. 12.1. Suggested scanning planes of the liver using the high acoustic power mode to detect focal liver lesions. The right liver is scanned in the transverse plane by one or two continuous sweeps, while the left liver is scanned in the longitudinal plane by one continuous sweep. If low acoustic power insonation is employed, the liver may be scanned on every plane since microbubble rupture is minimized.

continuously during the arterial (10–35 s), portal (40–90 s), and late (95–120 s from injection) phases, with multiple sweeps.

The low acoustic power mode presents several advantages in comparison with high acoustic power. First, it is easier to perform since the same region of the liver may be scanned more times due to the minimization of microbubble rupture. Second, more acoustic views (i.e., intercostal views) may be employed without evidence of significant artifacts, except for posterior acoustic shadowing of ribs. Third, the suppression of background signal from native stationary tissues is complete and the harmonic signal is produced almost completely from microbubble resonance.

12.1.3 Clinical Results

a) Comparison with baseline gray-scale US. In the comparative series with the largest patient numbers (Albrecht et al. 2001a, 2003a; Quaia et al. 2003), high acoustic power insonation was employed after air-filled microbubble injection. In these studies, contrast-enhanced US significantly improved (Figs. 12.2–12.4) the detection of liver metastases (from 47% to 56%) in comparison with baseline scan, and there was an improvement in sensitivity from 63–71% to 87–91%.

These results were achieved through the improved conspicuity (visibility) of metastatic lesions (Figs. 12.5, 12.6). In fact, during the late liver-specific phase, microbubbles spare metastases, which appear as hypovascular defects, while being selectively taken up by the adjacent liver parenchyma (Figs. 12.7, 12.8).

In livers containing metastases and appearing heterogeneous on baseline US, contrast-enhanced US reveals multiple (>5) metastatic lesions (Fig. 12.9). This is because even in the presence of extensive metastatic liver involvement, microbubbles accumulate in the interposed normal liver parenchyma, thereby increasing the visibility of metastases.

Additional metastatic liver lesions, identified after the injection of microbubble-based agents (Figs. 12.2–12.4, 12.8), usually measure less than 1 cm in diameter and are localized in the middle or anterior segment of the liver.

Contrast-enhanced US is most effective in detecting liver metastases in patients in whom metastases have already been identified on baseline US. On the other hand, in a study by Quaia et al. (2003), a small number of patients without evidence of metastatic liver lesions on the baseline scan were found to have one or more metastatic lesions after microbubble injection. Based on these results it seems reasonable to propose the employment of baseline US in patient follow-up after surgery, since state of the art US equipment with wideband transducers is sufficiently accurate in detecting liver metastases at the screening level. Contrast-enhanced US should be proposed in patients who show from one to five focal liver lesions suspected of being metastases on baseline US, the aim being to reveal additional metastatic lesions and to permit selection of the most suitable therapeutic approach (surgery, radiofrequency or palliative treatment if more than five metastatic lesions are identified; Robinson 2001).

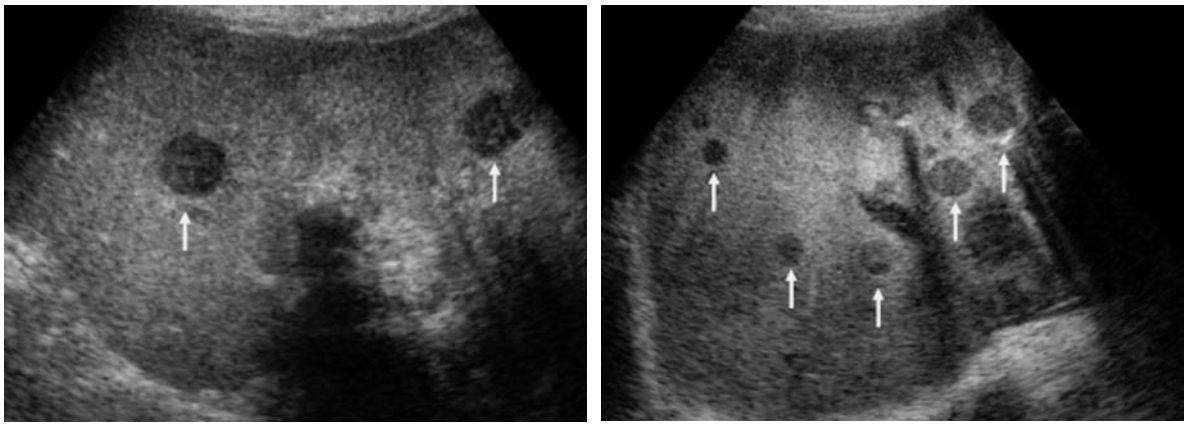

a b

Fig. 12.2a,b. Appearance of metastatic lesions in the late phase, 4 min after the injection of air-filled microbubbles, with high acoustic power insonation. The metastases appear as hypoechoic defects (*arrows*) in the enhancing liver.

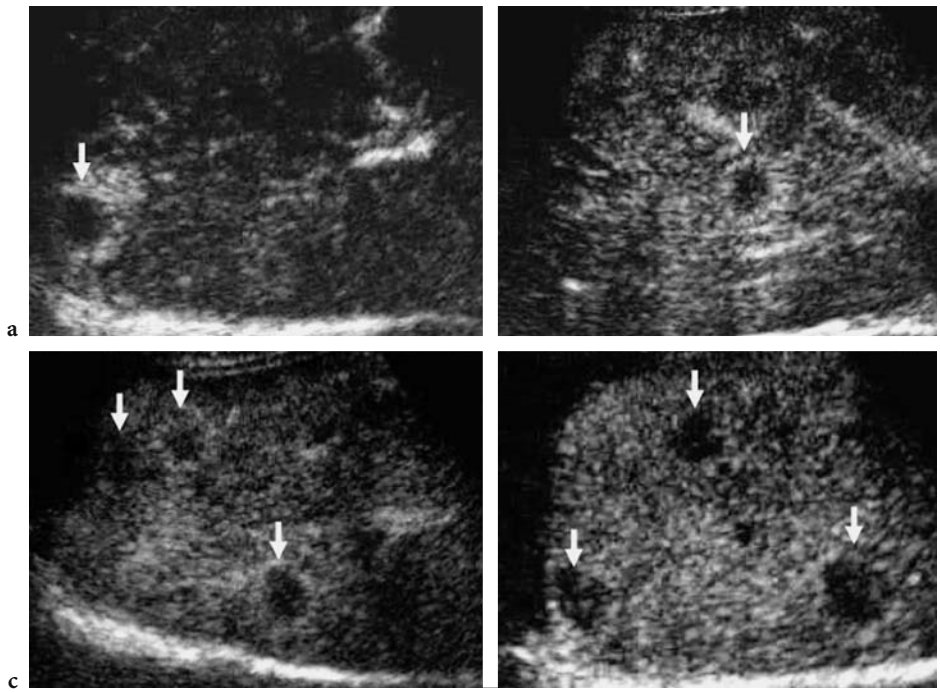

Fig. 12.3a–d. Appearance of metastatic lesions in the late phase, 110 s after the injection of sulfur hexafluoride-filled microbubbles, with low acoustic power insonation. The metastases appear as hypoechoic, hypovascular defects (*arrows*) in the normally enhancing adjacent liver.

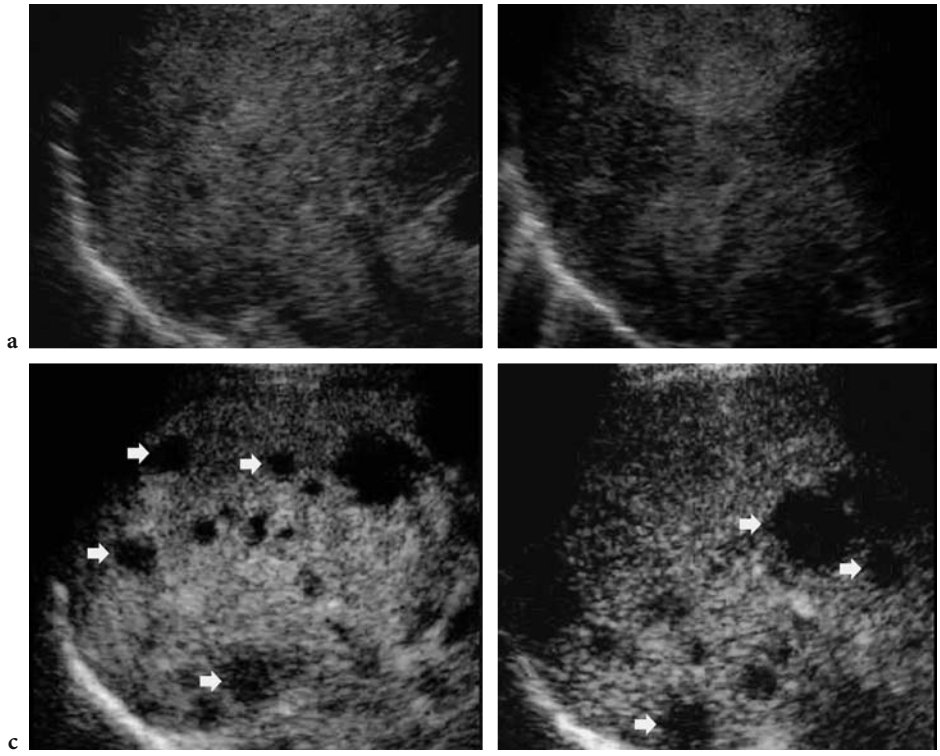

Fig. 12.4. a,b Heterogeneous appearance of the liver on baseline US. **c,d** Multiple metastases appear as hypoechoic defects (*arrows*) in the normally enhancing adjacent liver on contrast-enhanced US, 120 s after the injection of sulfur hexafluoride-filled microbubbles, with low acoustic power insonation.

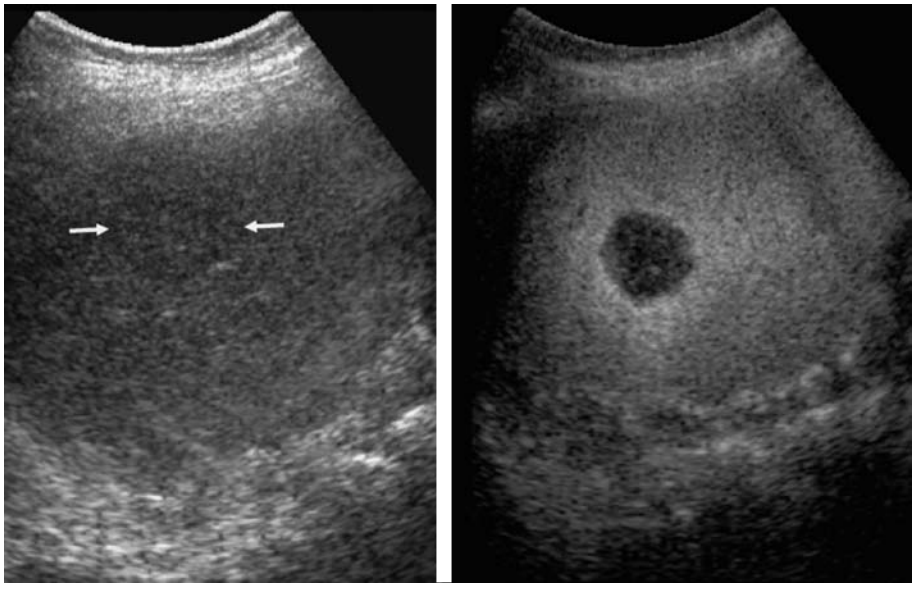

Fig. 12.5a,b. Improved metastatic lesion conspicuity on contrast-enhanced US in comparison with the baseline scan. High acoustic power mode after the injection of air-filled microbubbles. On baseline US (**a**) the metastatic lesion (*arrows*) is barely visible. The contrast between the metastatic lesion and the adjacent liver was clearly improved after microbubble injection (**b**).

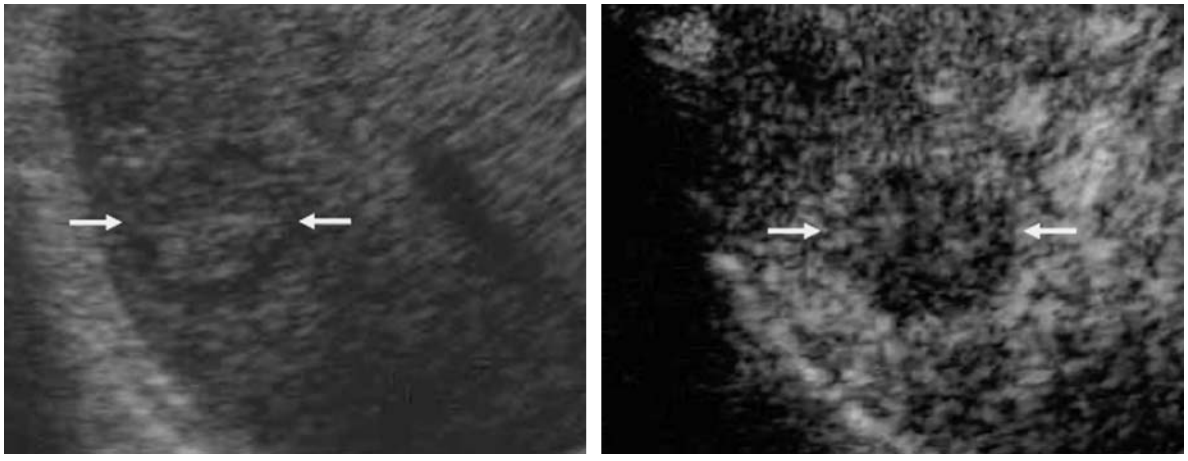

Fig. 12.6a,b. Improved metastatic lesion conspicuity on contrast-enhanced US (**b**) in comparison with the baseline scan (**a**). Low acoustic power mode after sulfur hexafluoride-filled microbubble injection. On baseline US (**a**) the metastatic lesion (*arrows*) presents a peripheral hypoechoic halo. The contrast between the metastatic lesion and the adjacent liver was clearly improved after microbubble injection (**b**).

b) Comparison with contrast-enhanced CT. Contrast-enhanced CT has been considered the reference standard in most of the published series (Quaia et al. 2003), sometimes with the addition of gadolinium-enhanced MR imaging (Albrecht et al. 2001a, 2003a). Nevertheless, contrast-enhanced CT cannot be considered a perfect tool for the detection of liver metastases (Robinson 2001).

Contrast-enhanced US shows a similar accuracy to contrast-enhanced CT in the detection of liver metastases (Fig. 12.10). A more important finding is that the additional metastatic lesions identified by contrast-enhanced US are predominantly less than a centimeter in diameter (Fig. 12.11) (Dalla Palma et al. 1999; Harvey et al. 2000a,b; Albrecht et al. 2001a; del Frate et al. 2003; Quaia et al. 2003). Moreover, the additionally detected liver metastases are mainly located in the middle and anterior segments of the liver (Fig. 12.12), since the contrast enhancement after the injection of microbubble-based agents is

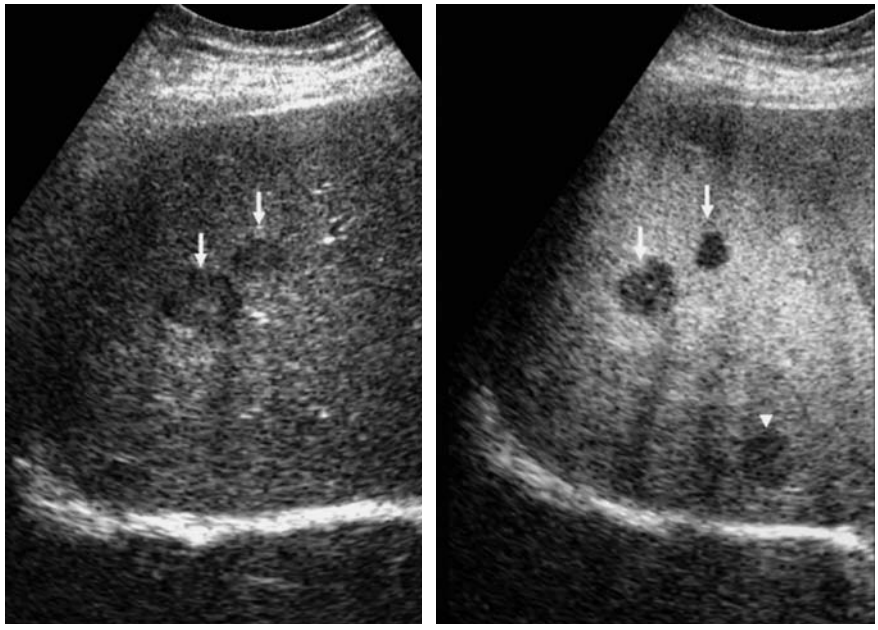

Fig. 12.7a,b. Improved lesion detection by contrast-enhanced US in comparison with the baseline scan. High acoustic power mode after the injection of air-filled microbubbles. Two focal liver lesions (*arrows*) are identified on the baseline scan (**a**). An additional focal liver lesion (*arrowhead*) is identified in the liver segment close to the diaphragm after microbubble injection (**b**).

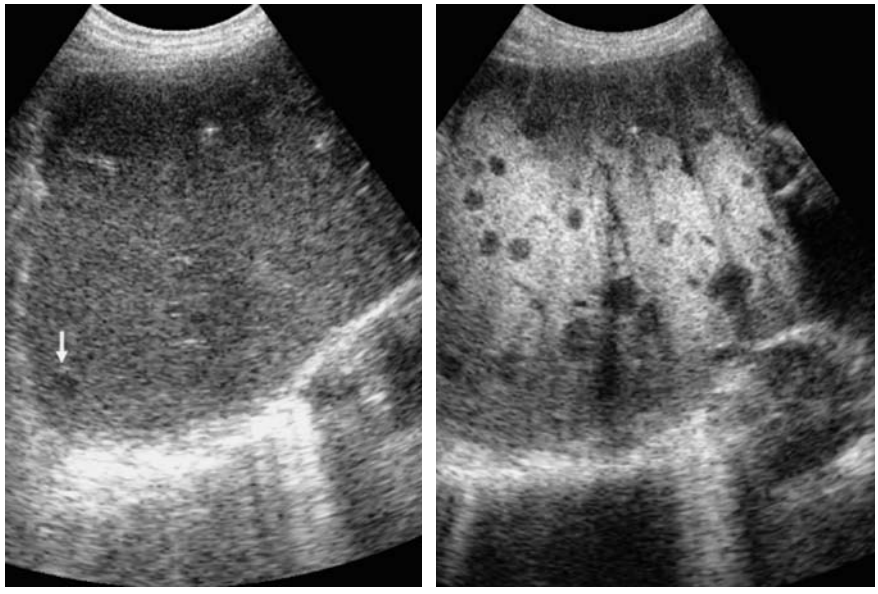

Fig. 12.8a,b. Improved lesion detection by contrast-enhanced US in comparison with the baseline scan. High acoustic power mode after air-filled microbubble injection. Only one metastatic lesion (*arrow*) can be identified on the baseline scan (**a**), while contrast-enhanced US (**b**) reveals multiple metastatic lesions.

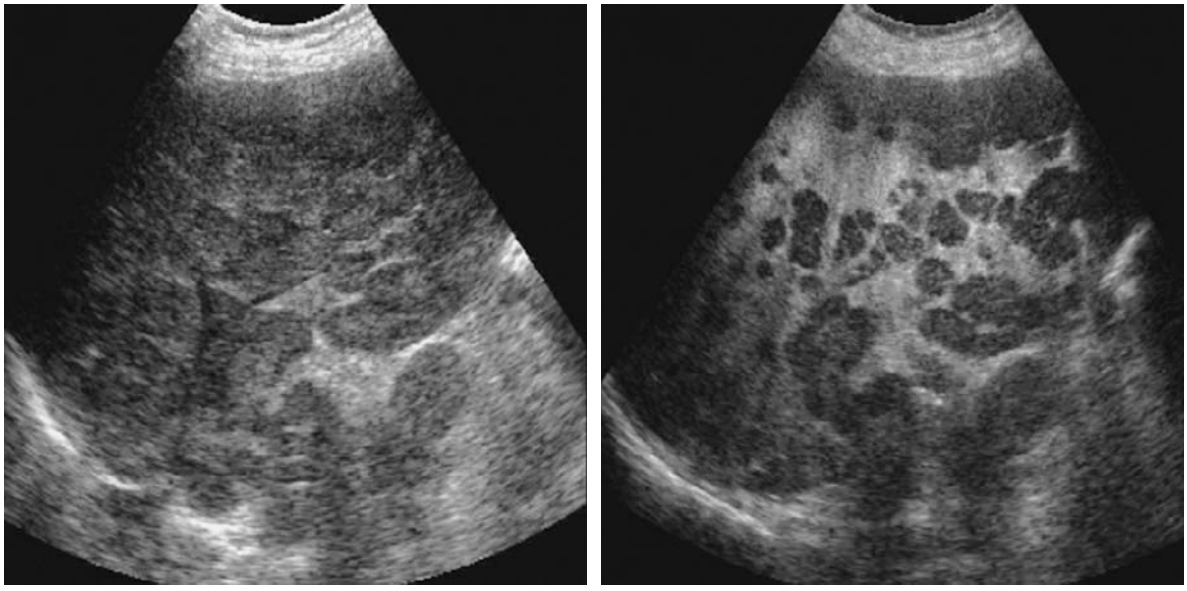

a **b**

Fig. 12.9a,b. Improved detection of metastatic lesions by contrast-enhanced US (**b**) in comparison with baseline US (**a**). High acoustic power mode after air-filled microbubble injection. A heterogeneous appearance of liver parenchyma is identified on the baseline scan (**a**). Multiple metastatic lesions are identified after microbubble injection in the late phase (**b**).

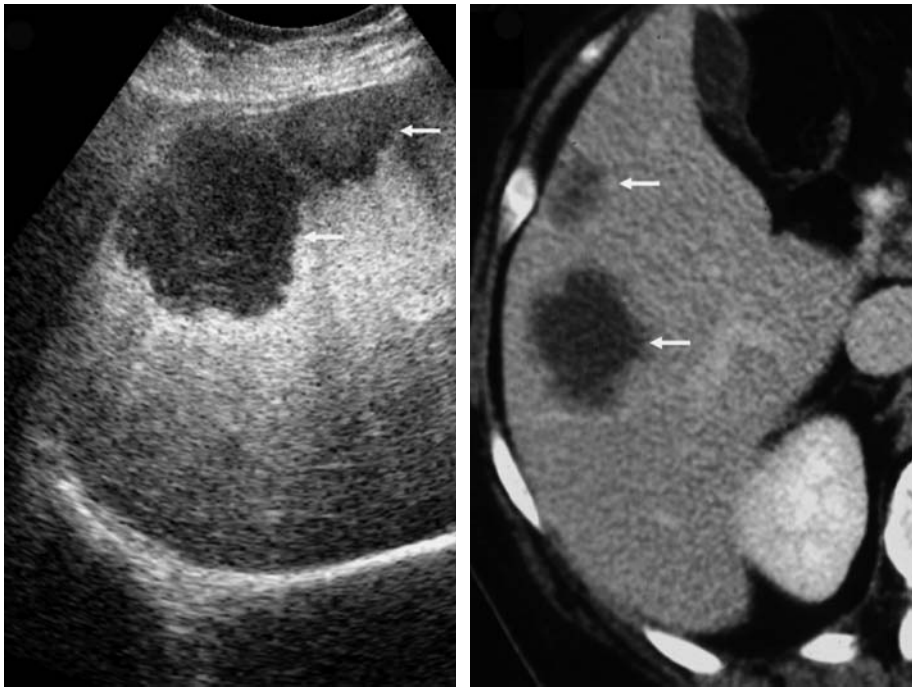

a **b**

Fig. 12.10a,b. Similar accuracy of contrast-enhanced US and contrast-enhanced CT in the detection of metastatic lesions. Two liver metastases (*arrows*) are identified on contrast-enhanced US (**a**) and confirmed on contrast-enhanced CT (**b**). High acoustic power mode after air-filled microbubble injection.

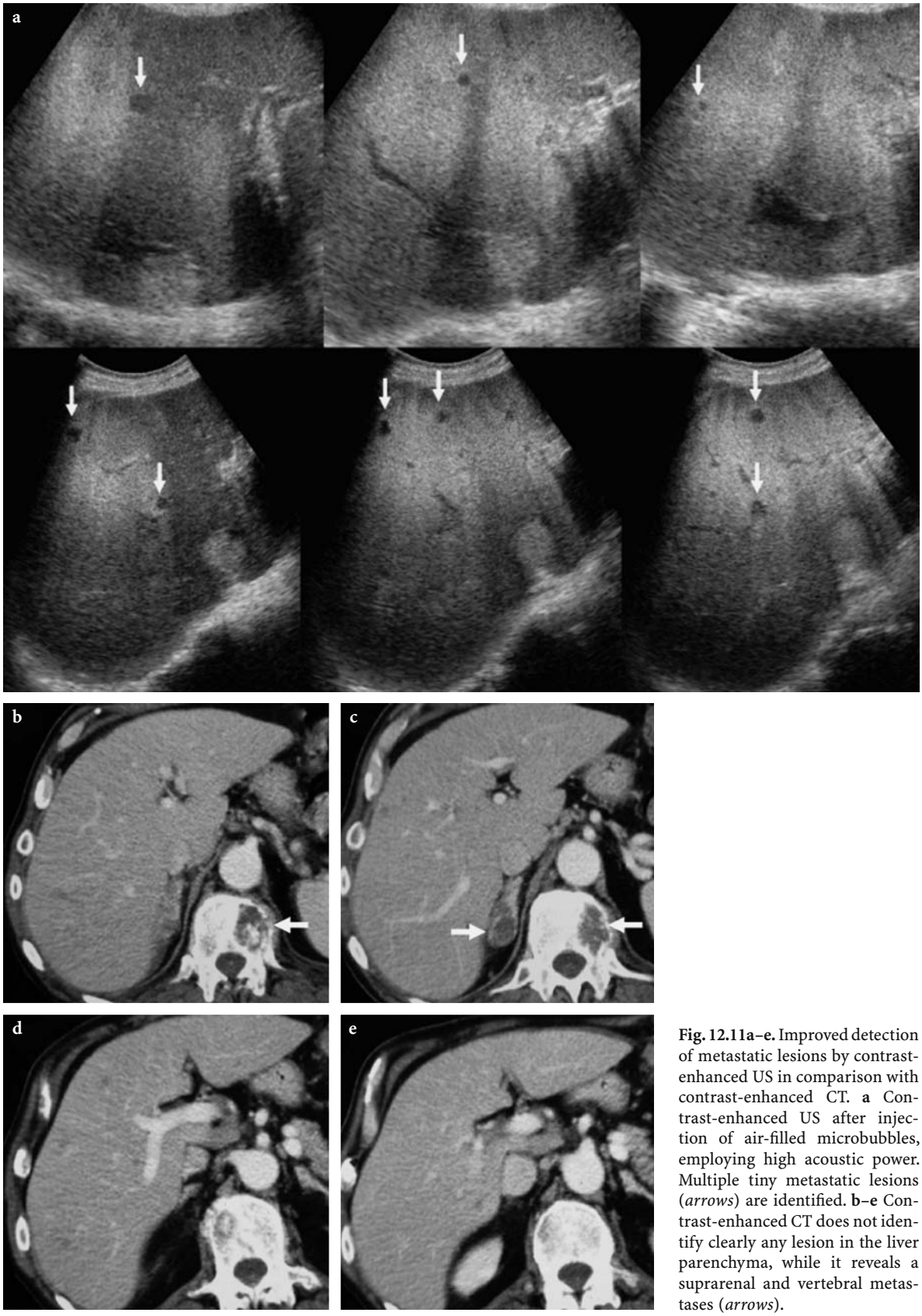

Fig. 12.11a–e. Improved detection of metastatic lesions by contrast-enhanced US in comparison with contrast-enhanced CT. **a** Contrast-enhanced US after injection of air-filled microbubbles, employing high acoustic power. Multiple tiny metastatic lesions (*arrows*) are identified. **b–e** Contrast-enhanced CT does not identify clearly any lesion in the liver parenchyma, while it reveals a suprarenal and vertebral metastases (*arrows*).

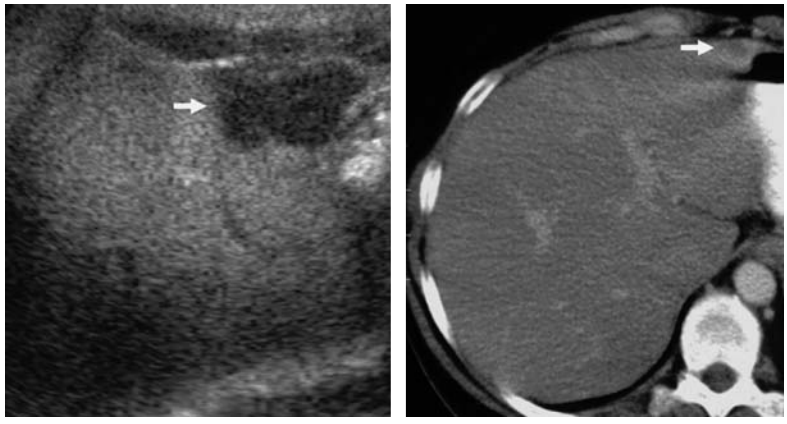

Fig. 12.12a,b. Improved detection of metastatic lesions by contrast-enhanced US in comparison with contrast-enhanced CT. Contrast-enhanced US (**a**) after the injection of air-filled microbubbles, with high acoustic power. A single metastasis is identified in the anterior region of the left liver lobe. This lesion (*arrow*) was identified only retrospectively on contrast material-enhanced CT (**b**).

most intense above the focal zone (Albrecht et al. 2000), where the intensity of the beam is higher and the microbubble destruction more extensive.

Contrast-enhanced US does, however, have clear limitations in the detection of liver metastases in liver segments close to the diaphragm and inferior vena cava (Fig. 12.13) (Quaia et al. 2003) and in liver regions hidden by the posterior acoustic shadowing from the bowel gas (Fig. 12.14). The limited value of contrast-enhanced US in the assessment of deep liver segments is principally due to the deep position of the focal zone, which prevents homogeneous and effective bubble rupture throughout liver parenchyma. In fact, even though the deep liver segments are near the focal zone, these segments are the most difficult to assess by contrast-enhanced US since the broadband signal from microbubble destruction is extensively attenuated by superficial planes.

c) Comparison with Gd-enhanced or SPIO-enhanced MR. MR imaging has become an important tool in clinical liver imaging thanks to the introduction of faster imaging techniques. The advent of liver-specific MR imaging contrast materials, which are

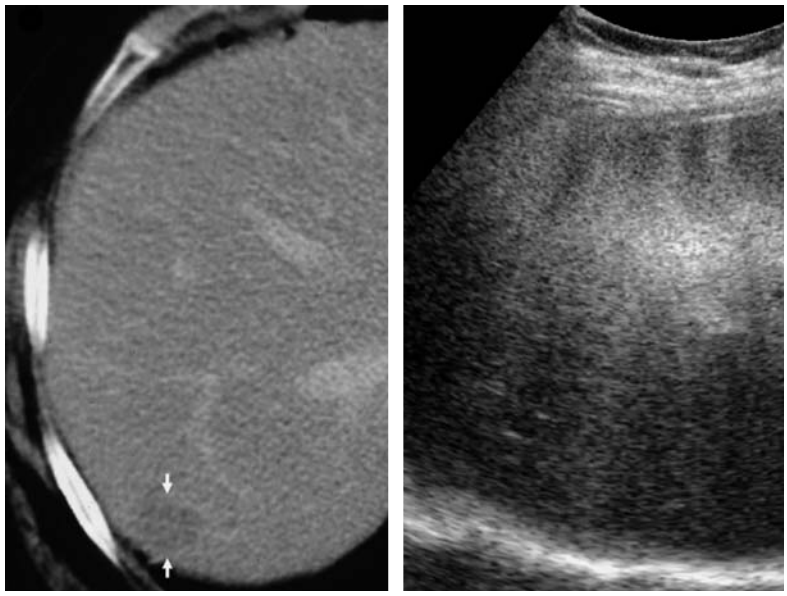

Fig. 12.13a,b. Improved lesion detection on contrast-enhanced CT in comparison with contrast-enhanced US. A single, very deeply located metastatic lesion (*arrows*) is seen on contrast-enhanced CT (**a**), while contrast-enhanced US (high acoustic power mode after air-filled microbubble injection) (**b**) does not identify any lesion.

agents targeted at the enhancement of hepatocytes or Kupffer cells, has facilitated an increase in the accuracy of MR imaging in liver metastasis detection (del Frate et al. 2002). In series with Gd-BOPTA- (Mosconi et al. 2003) or SPIO-enhanced MR (del Frate et al. 2003) as the reference standards, similar results were observed to those using CT as the reference standard, with similar limitations for contrast-enhanced US (Figs. 12.15–12.18).

d) Contrast-enhanced intraoperative US. Dedicated intraoperative US transducers equipped with contrast-specific US modes are available and may be employed after microbubble injection to improve the

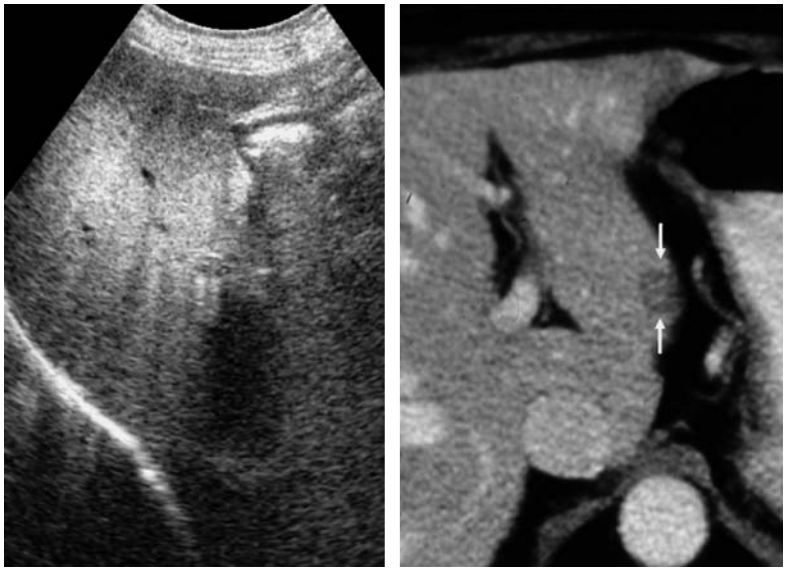

Fig. 12.14a,b. Improved lesion detection on contrast-enhanced CT in comparison with contrast-enhanced US. **a** Contrast-enhanced US was performed employing the high acoustic power mode after air-filled microbubble injection. No lesion is identified in the liver. **b** Contrast-enhanced CT during the portal phase. A single metastatic lesion (*arrows*) is identified behind the stomach.

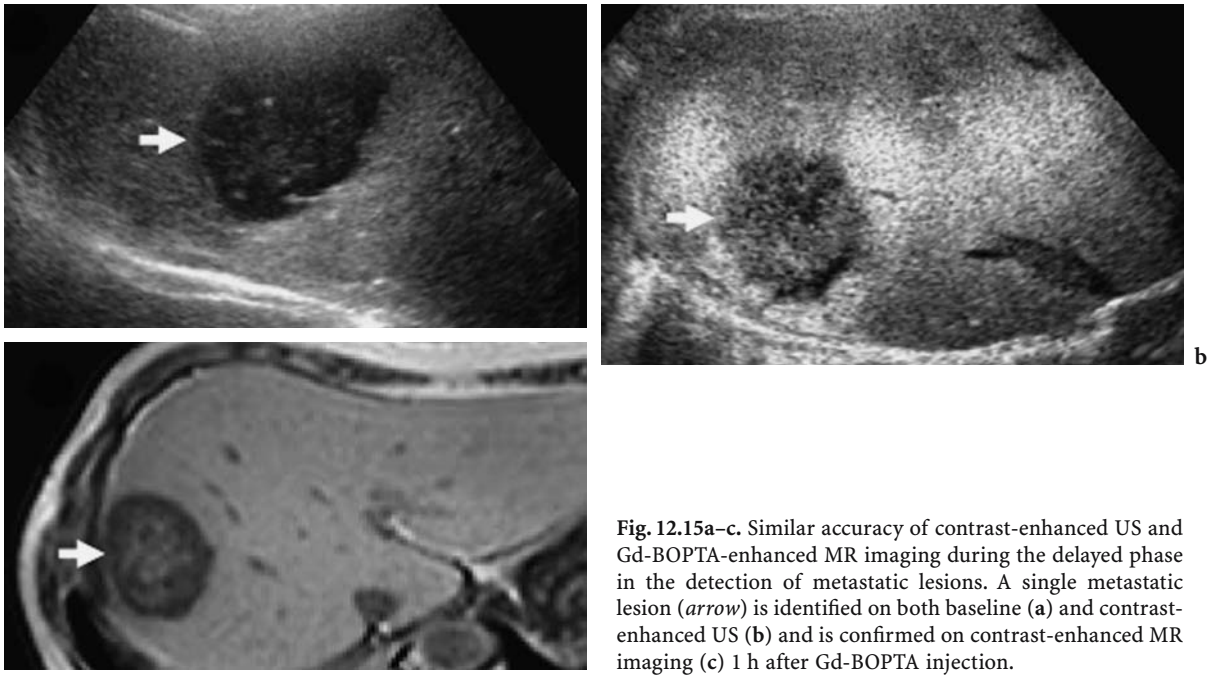

Fig. 12.15a–c. Similar accuracy of contrast-enhanced US and Gd-BOPTA-enhanced MR imaging during the delayed phase in the detection of metastatic lesions. A single metastatic lesion (*arrow*) is identified on both baseline (**a**) and contrast-enhanced US (**b**) and is confirmed on contrast-enhanced MR imaging (**c**) 1 h after Gd-BOPTA injection.

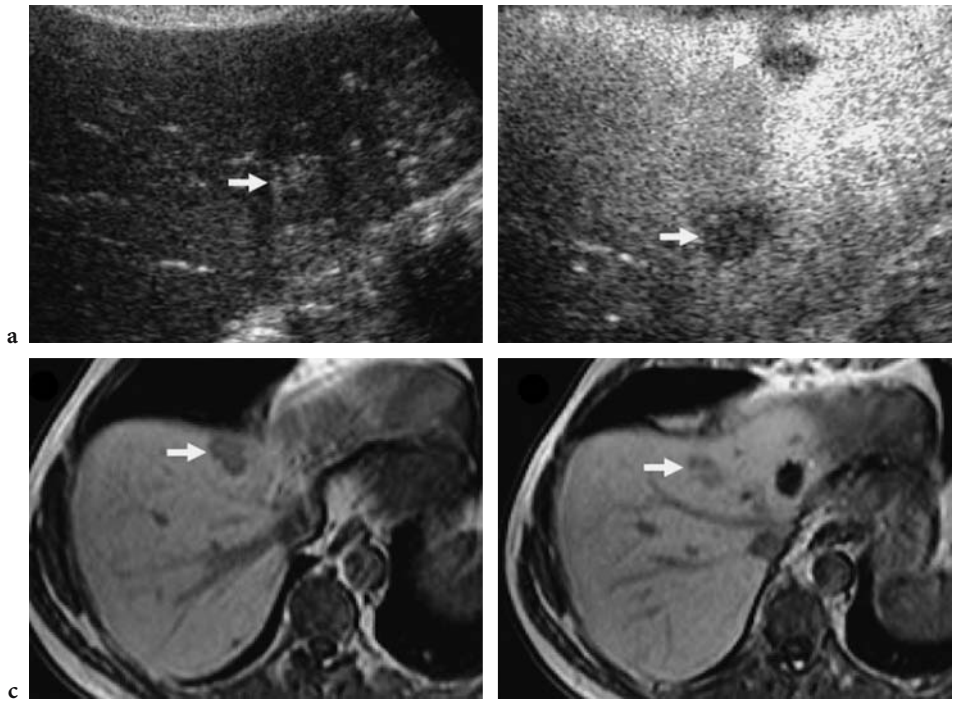

Fig. 12.16a–d. Improved lesion detection by contrast-enhanced US in comparison with Gd-BOPTA-enhanced MR imaging in the delayed phase. **a, b** A single metastatic lesion (arrow) is identified by baseline US (**a**), while contrast-enhanced US (high acoustic power mode after air-filled microbubble injection) (**b**) identifies one additional lesion. **c, d** Contrast-enhanced MR imaging performed 1 h after Gd-BOPTA injection confirms only the first lesion (*arrow*).

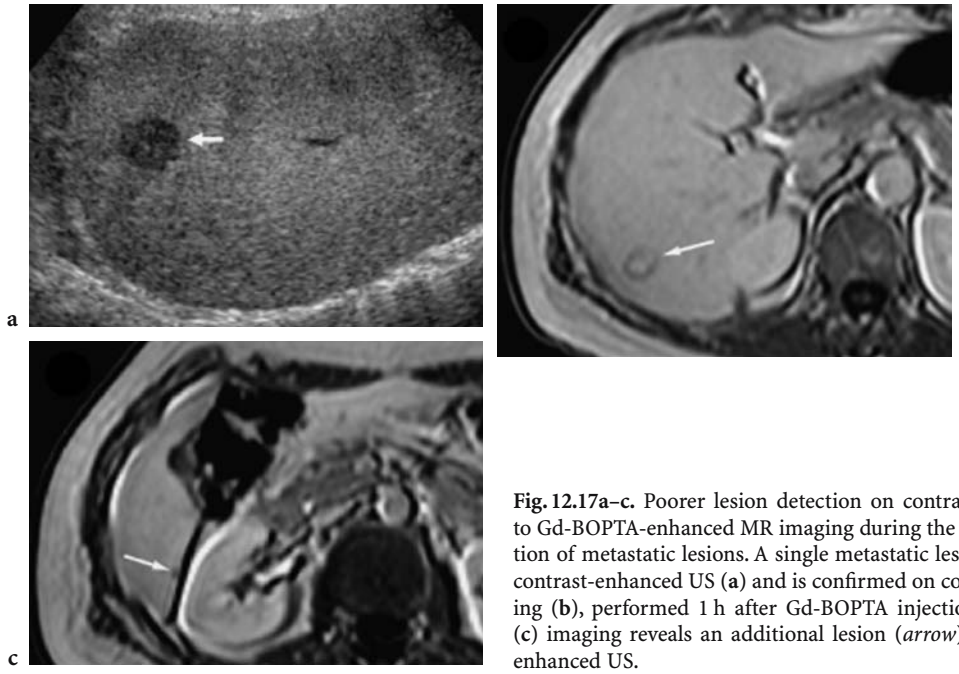

Fig. 12.17a–c. Poorer lesion detection on contrast-enhanced US compared to Gd-BOPTA-enhanced MR imaging during the delayed phase in the detection of metastatic lesions. A single metastatic lesion (*arrow*) is identified by contrast-enhanced US (**a**) and is confirmed on contrast-enhanced MR imaging (**b**), performed 1 h after Gd-BOPTA injection. Contrast-enhanced MR (**c**) imaging reveals an additional lesion (*arrow*) not detected by contrast-enhanced US.

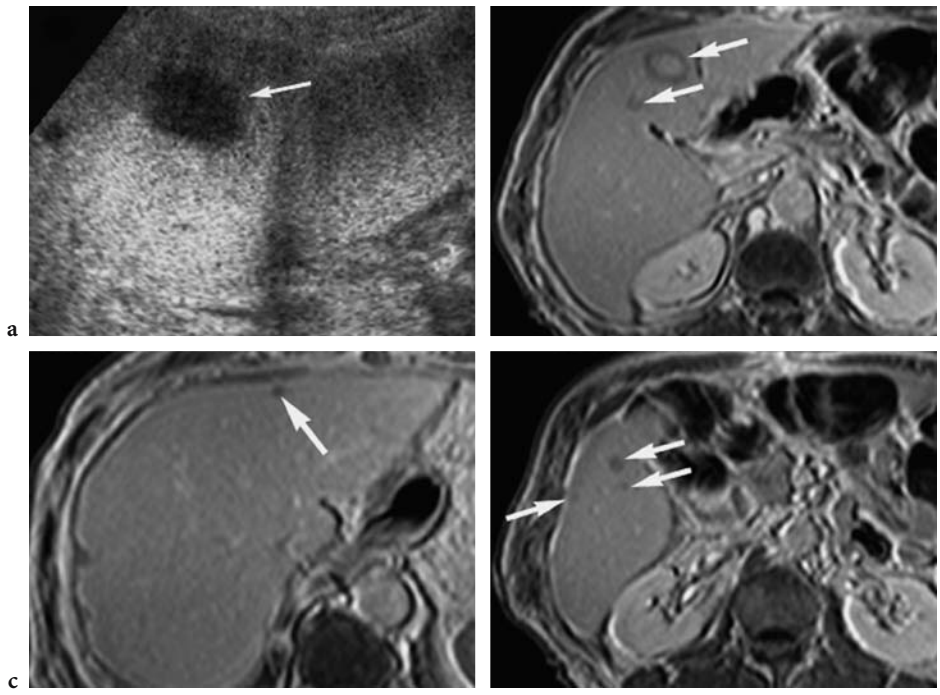

Fig. 12.18a–d. Poorer lesion detection on contrast-enhanced US in comparison with Gd-BOPTA-enhanced MR in the delayed phase. A single metastatic lesion (*arrow*) is identified by contrast-enhanced US in the high acoustic power mode after air-filled microbubble injection (**a**), while contrast-enhanced MR, performed 1 h after Gd-BOPTA injection, confirms the previous lesion (**b**) and reveals multiple additional tiny lesions (**c, d**; *arrows*)

detection of liver metastases (Fig. 12.19). Intraoperative US allows placement of the transducer directly at the liver surface, avoiding the limitations due to bowel gas interposition or a large body habitus. This further improves liver metastasis detection as compared to transabdominal contrast-enhanced US.

e) Limitations of contrast-enhanced US. The real advantage of contrast-enhanced US in the detection of liver metastases is evident in patients with optimal visibility of the liver parenchyma. Contrast-enhanced US has the same limitations as conventional US when there is bowel gas interposition or when the patient has a large body habitus (Quaia et al. 2003). The effectiveness of contrast-enhanced US is also limited in patients with steatotic or cirrhotic liver parenchyma: it is in such patients that the lowest liver parenchyma enhancement and the poorest visibility of metastases has been observed (Quaia et al. 2003). This is because in such patients the liver parenchyma appears diffusely hyperechoic even on baseline US and contrast enhancement is difficult to visualize. This limitation is overcome by low acoustic power insonation with new-generation perfluorocarbon- or sulfur hexafluoride-filled microbubbles, which allow good suppression of the background from stationary tissues.

The second important limitation of contrast-enhanced US is the possibility of false positive findings, corresponding to lesions which are not actually present and not confirmed by the reference standards (Quaia et al. 2003). Moreover, some benign focal liver lesions, such as atypical sclerotic liver hemangioma and focal fatty changes, may simulate liver metastases on contrast-enhanced US (Fig. 12.20) since they sometimes appear as hypovascular defects in the liver-specific late phase (Bertolotto et al. 2000; Quaia et al. 2002a, 2003); this is especially true for hemangiomas that present a thrombotic pattern or focal fatty changes with a predominant fat component. In addition, artifacts from heterogeneous microbubble rupture appear as hypovascular echoic focal zones and may simulate focal liver lesions on contrast-enhanced US (Fig. 12.21) (Quaia et al. 2003).

12.2 Detection of Hepatocellular Carcinoma

In chronic diffuse liver disease, macroregenerative nodules and hepatocellular carcinomas are the most characteristic and frequently observed focal liver

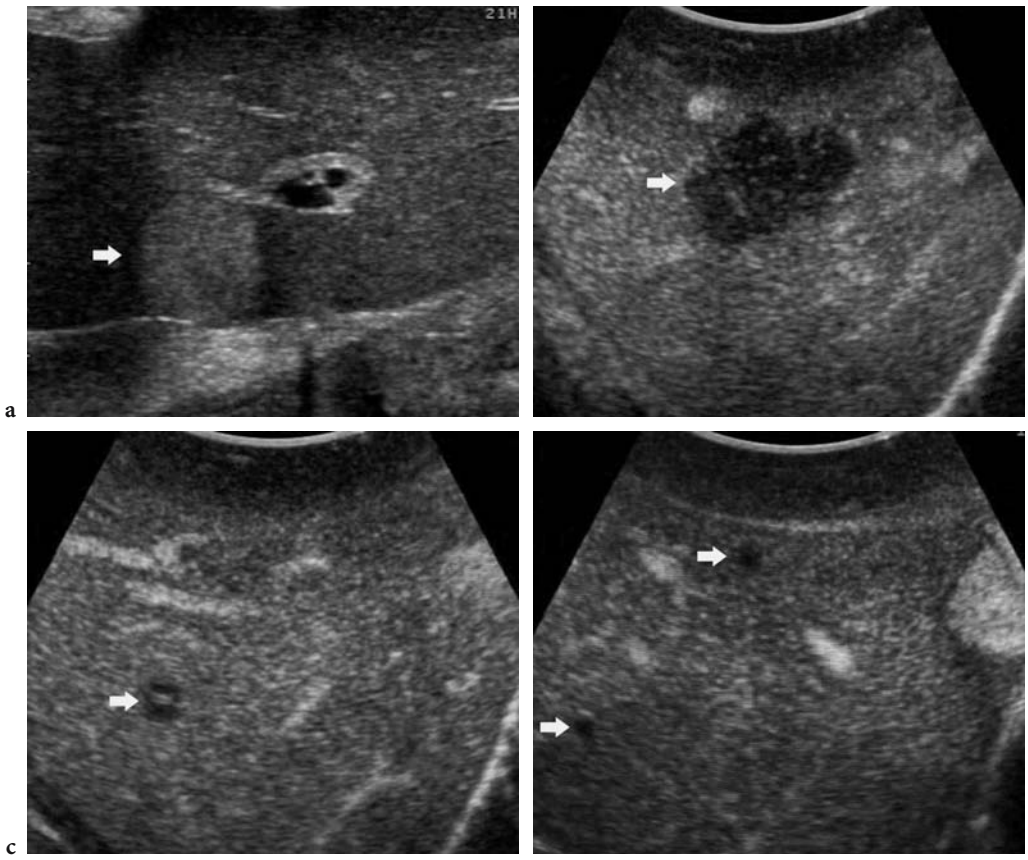

Fig. 12.19. a Baseline intraoperative US identifies one liver metastasis (*arrow*). **b–d** Dedicated intraoperative US transducer equipped with contrast-specific modes; images obtained 90 s after microbubble-based agent injection. The liver metastatic lesion (*arrow*) identified by baseline US is confirmed after microbubble-based agent injection (**b**). Further subcentimeter metastatic lesions (*arrows*) are identified after microbubble injection (**c, d**). Courtesy of Dr. Roberta Padovan, Aloka, Japan.

lesions (Baron and Peterson 2001), while hemangiomas and focal nodular hyperplasia are occasionally observed. Each focal liver lesion identified in a cirrhotic patient has to be considered a hepatocellular carcinoma until proven otherwise. The detection of hepatocellular carcinoma in patients with cirrhosis has been considered a technical challenge (Laghi et al. 2003) because cirrhosis alters both liver parenchymal characteristics (through fibrosis, the development of regenerative nodules, and fatty infiltration) and vascularization (through portal hypertension and the creation of arterial–portal venous shunts).

a) Detection by baseline US. The detection of hepatocellular carcinoma by baseline US is related to the size, echogenicity, and location of lesions and to the experience of the sonologist. Baseline US has a detection rate from 46% to 95% for lesions smaller than 2 cm (Takayasu et al. 1990; Harvey and Albrecht 2001a; Solbiati et al. 2001) and from 13% to 37% for lesions smaller than 1 cm (Solbiati et al. 2001). The highest detection rates are achieved for hypoechoic lesions with a peripheral halo and the lowest rates for hyperechoic lesions without a peripheral halo. Multifocality is very frequent in hepatocellular carcinoma, occurring in about 80% of patients (Solbiati et al. 2001). The low sensitivity of baseline US is principally caused by the presence of heterogeneous and attenuating liver echotexture due to cirrhotic distortion and focal fibrosis.

b) Detection by cross-sectional imaging techniques. The reported sensitivity in the detection of hepatocellular carcinomas smaller than 3 cm is 46–88% for contrast-enhanced multiphase CT, 61–81% for angiography, 86–91% for CT arterial portography, 71–96% for iodized oil CT, and 94–96% for intraoperative US (Choi et al. 1989, 1991; Takayasu et al. 1990; Solbiati et al. 2001; Laghi et al. 2003).

The principal reason for the limited sensitivity of CT is the presence of cirrhotic distortion and focal

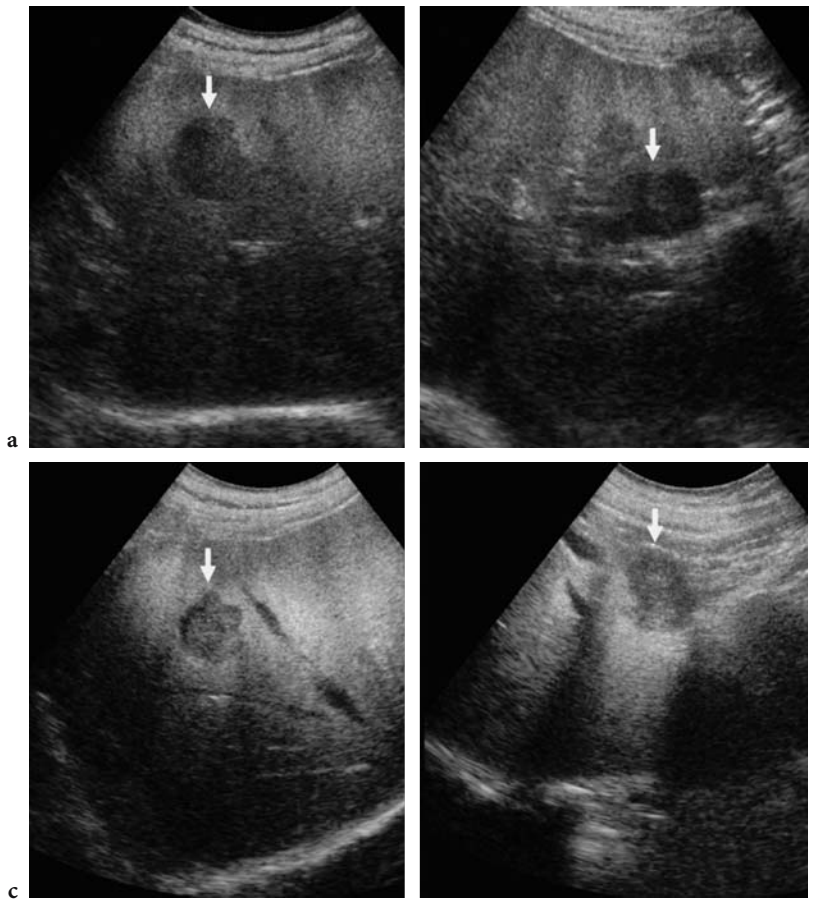

Fig. 12.20a–d. False positive findings of contrast-enhanced US. High acoustic power mode after air-filled microbubble injection. A focal liver lesion (*arrow*) appears hypoechoic on contrast-enhanced US during the late phase (**a, b**) and was considered to be a metastasis. US-guided biopsy revealed a sclerotic hemangioma which appeared unchanged at follow-up, also performed by contrast-enhanced US (**c, d**).

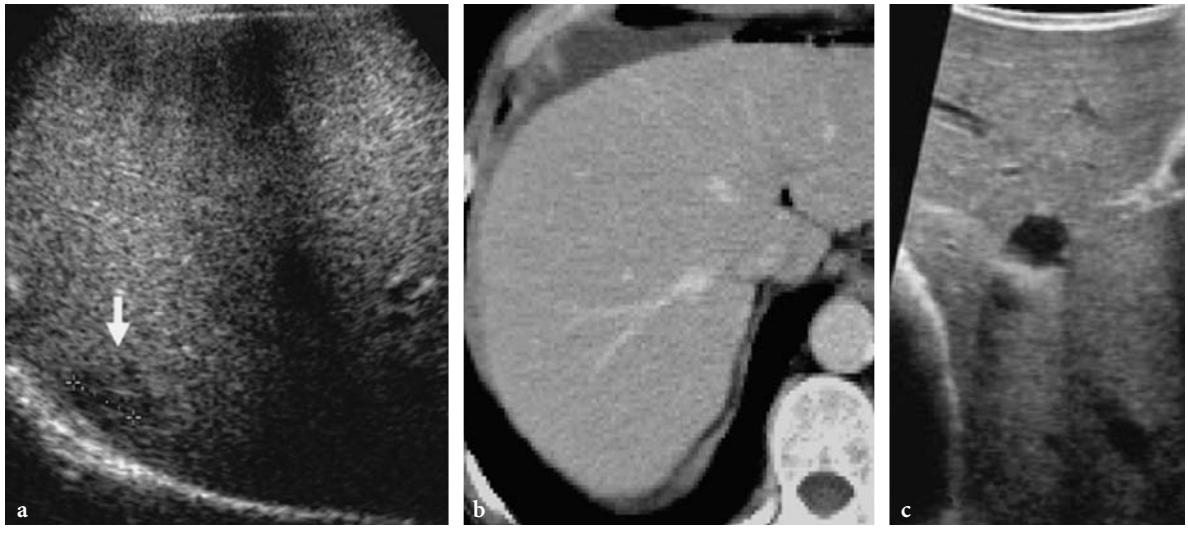

Fig. 12.21a–c. False positive findings of contrast-enhanced US. A focal liver lesion (*arrow*) that was deeply located and hypoechoic on contrast (Levovist)-enhanced US during the late phase (**a**) was considered to represent a metastasis. Contrast-enhanced CT (**b**) and intraoperative US (**c**) did not confirm this finding, which was considered an artifact due to heterogeneous microbubble rupture.

fibrosis, leading to heterogeneous contrast enhancement in the liver parenchyma. Focal liver lesions may be simulated by wedge-shaped areas that are widest at the capsular surface and are frequently associated with liver parenchymal atrophy and capsular retraction. The differentiation from real focal liver lesions is further hindered by the fact that focal liver fibrosis may display enhancement on contrast-enhanced CT (Baron and Peterson 2001). Moreover, besides cirrhotic distortion of liver parenchyma and focal fibrosis, other types of focal liver parenchymal or vascular abnormalities may simulate focal liver lesions. In fact, it was shown that approximately one-third of the false positive diagnoses of hepatocellular carcinoma made with screening contrast-enhanced CT in a large transplantation series were due to enhancing vascular lesions, such as hemangioma, small arteriovenous shunts, and pseudoaneurysms (Baron and Peterson 2001).

New diagnostic procedures, such as single- or double-contrast, Gd- and/or SPIO-enhanced MR imaging, have been reported to offer good diagnostic confidence and sensitivity in the detection of hepatocellular carcinoma (Yamashita et al. 1996; Ward et al. 2000a,b, 2003; Pauleit et al. 2002; Kang et al. 2003; Teefey et al. 2003), with a lower percentage of false positive findings.

c) Detection by contrast-enhanced US. Since cirrhotic liver parenchyma shows diffusely heterogeneous contrast enhancement after microbubble injection due to the fibrotic component (Quaia et al. 2002c), contrast-enhanced US cannot be considered a reliable method for the detection of focal liver lesions in cirrhotic patients. The heterogeneous contrast enhancement due to fibrotic changes may simulate multiple focal liver lesions (Fig. 12.22). Persistent microbubble uptake during the late phase in some hepatocellular carcinoma nodules makes detection even more difficult (Quaia et al. 2002c, 2004). The performance of contrast-enhanced US is better in hepatocellular carcinoma nodules with a hypovascular appearance in the late phase (Figs. 12.23, 12.24).

The low acoustic power mode with new-generation microbubble-based contrast agents seems to

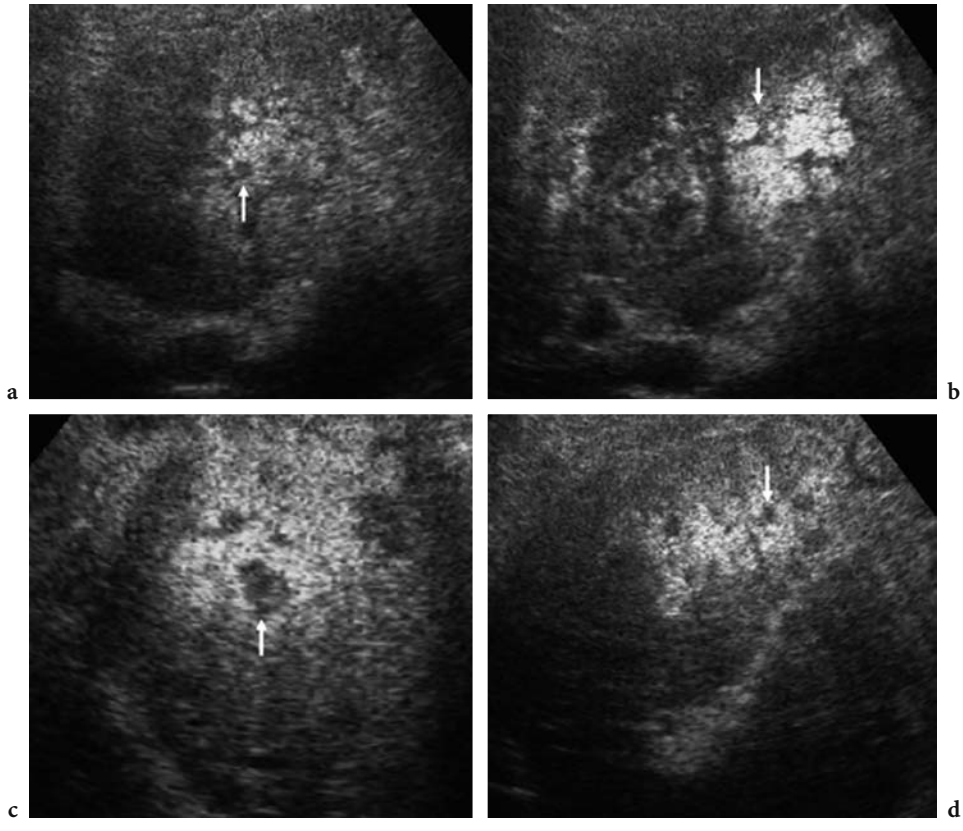

Fig. 12.22a–d. False positive findings of contrast-enhanced US in the cirrhotic liver during the late phase following air-filled microbubble injection. The diffusely heterogeneous contrast enhancement in the cirrhotic liver parenchyma simulates multiple focal liver lesions (*arrows*). The hypoechoic regions in the liver parenchyma are instead due to focal fibrotic changes.

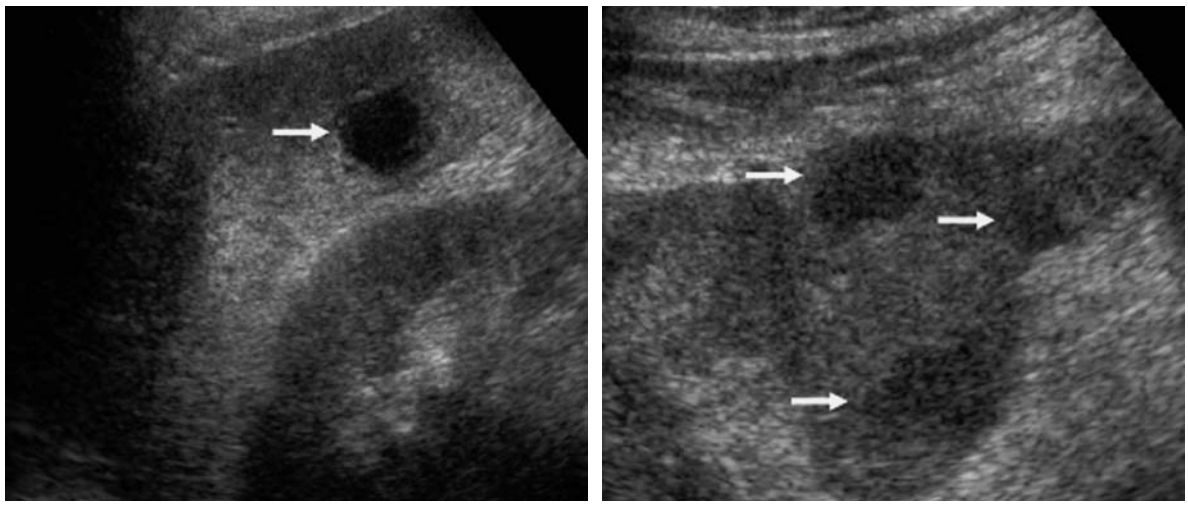

Fig. 12.23a,b. Improved hepatocellular carcinoma detection by contrast-enhanced US in comparison with the baseline US scan. High acoustic power mode after air-filled microbubble injection. One focal liver lesion (*arrows*) is identified on the baseline scan (**a**). Two additional tiny focal liver lesions (*arrowheads*) are identified in the liver after microbubble injection (**b**).

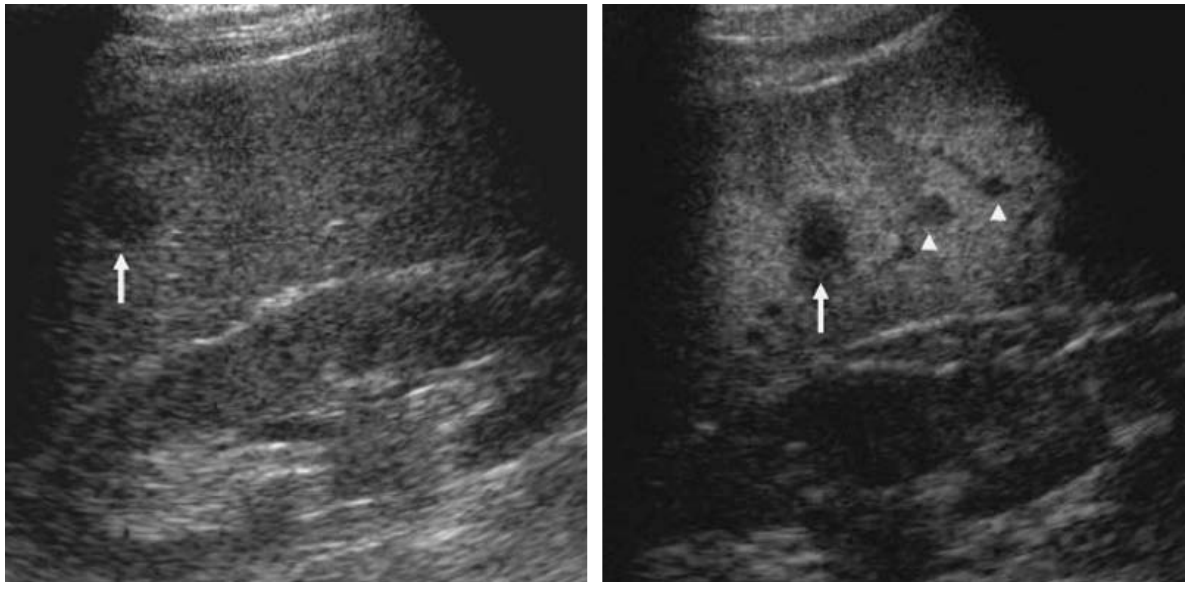

Fig. 12.24a,b. Evidence of multifocal hepatocellular carcinoma in the late phase, 4 min after air-filled microbubble injection and high acoustic power insonation. Multiple hypovascular lesions (*arrows*) are identified in the liver parenchyma. . Courtesy of Prof. M.J.K. Blomley, London, UK.

have improved the detection of hepatocellular carcinomas, primarily because it allows assessment of the liver parenchyma during each dynamic phase (Solbiati et al. 2000, 2001). Assessment should be performed both during the arterial phase to improve the detection of hypervascular lesions and during the late phase to enhance the detection of hepatocellular carcinomas that have a hypoechoic appearance in this phase (Fig. 12.25).

12.3 When Should Microbubble-Based Agents Be Employed?

Microbubble-based agents have been found to be very effective in facilitating the detection of liver metastases, especially subcentimeter lesions (Dalla Palma et al. 1999; Harvey et al. 2000a,b; Albrecht et al. 2001a; del Frate et al. 2003; Quaia et al.

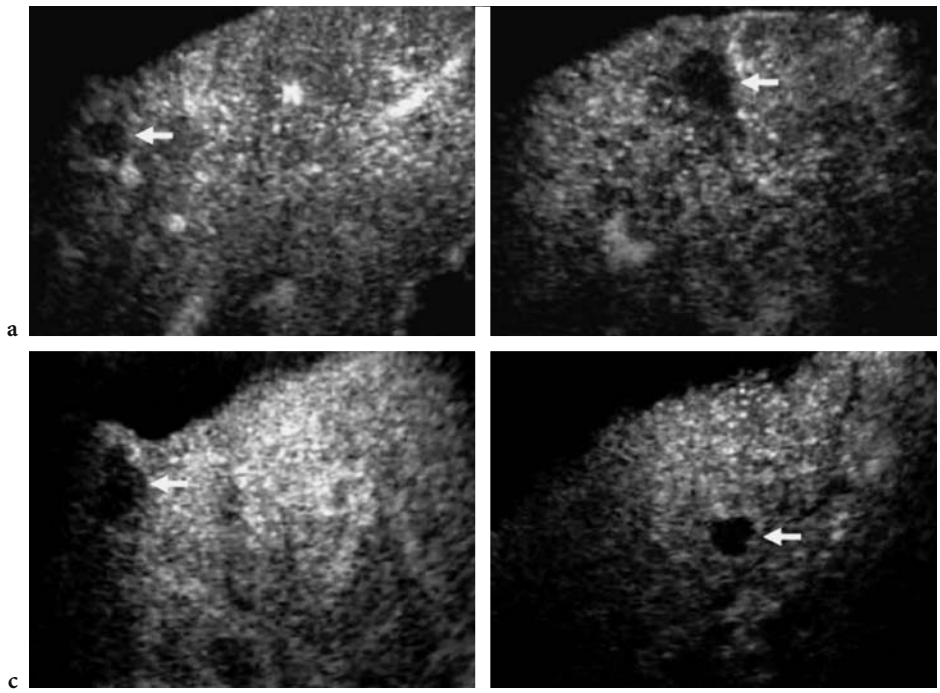

Fig. 12.25a–d. Evidence of multifocal hepatocellular carcinoma in the late phase, 90 s after the injection of sulfur hexafluoride-filled microbubbles, with low acoustic power insonation. Single hepatocellular carcinoma nodules appear as hypoechoic defects (*arrows*) in the enhancing adjacent cirrhotic liver parenchyma.

2003). Nevertheless, contrast-enhanced US has the same limitations as baseline US for the evaluation of liver parenchyma in patients with high-grade liver steatosis, a large body habitus, or interposing bowel gas. For these reasons, microbubble-based agents should be employed only in patients with a satisfactory liver parenchyma assessment at baseline US.

Moreover, since contrast-enhanced US has been found useful in identifying additional liver metastases in patients with one to three lesions, suspicious lesions, or heterogeneous liver parenchyma on baseline US (Quaia et al. 2003), microbubbles should not be employed in patients with a normal liver parenchyma on baseline US. Nowadays, state of the art US equipment allows reliable assessment of liver parenchyma on the baseline scan, including with the aid of speckle-reducing techniques such as tissue harmonic and compound imaging. Patients who are positive for or are suspected of having liver metastases at baseline US can be accurately assessed after microbubble injection. This technique can assist in the decision on whether to employ conservative or palliative treatment, depending on whether fewer or more than five metastases are detected.

References

Albrecht T, Hoffmann CW, Schettler S et al (2000) B-mode enhancement using phase inversion US with air-based microbubble contrast agent: initial experience in humans. Radiology 216:273-278

Albrecht T, Hoffmann CW, Schmitz SA et al (2001a) Phase inversion sonography during the liver specific late phase of contrast enhancement: improved detection of liver metastases. Am J Roentgenol 176:1191-1198

Albrecht T, Needleman L, Blomley MJ et al (2001b) Detection of focal liver lesions with the new US contrast agent NC100100: results of an exploratory multicentre study. Eur Radiol 11 [Suppl 1]:213

Albrecht T, Blomley MJK, Burns P et al (2003a) Improved detection of hepatic metastases with Pulse-Inversion US during the liver-specific phase of SHU 508A: multicenter study. Radiology 227:361-370

Albrecht T, Oldenburg A, Hohmann J et al (2003b) Imaging of liver metastases with contrast-specific low-MI real time ultrasound and SonoVue. Eur Radiol 13 [Suppl 3]:N79-N86

Baron RL, Peterson MS (2001) Screening the cirrhotic liver for hepatocellular carcinoma with CT and MR imaging: opportunities and pitfalls. Radiographics 21:S117-S132

Bauer A, Blomley MJK, Leen E et al (1999) Liver-specific imaging with SH U563A: Diagnostic potential of a new class of ultrasound contrast media. EUR Radiol 9 [Suppl 3]: S349–S352

Bellin MF, Zaim S, Auberton E (1994) Liver metastases: safety

and efficacy of detection with superparamagnetic iron oxide in MR imaging. Radiology 193:657-663

Bertolotto M, Dalla Palma L, Quaia E, Locatelli M (2000) Characterization of unifocal liver lesions with pulse inversion harmonic imaging after Levovist injection: preliminary results. Eur Radiol 10:1369-1376

Blomley MJK, Albrecht T, Cosgrove DO et al (1998) Stimulated acoustic emission in liver parenchyma with Levovist. Lancet 351:568-569

Blomley MJ, Albrecth TA, Cosgrove DO et al (1999) Improved detection of liver metastases with stimulated acoustic emission in late phase of enhancement with the US contrast agent SH U 508: early experience. Radiology 210:409-416

Carter R, Hemingway D, Pickard R et al (1996) A prospective study of six method for detection of hepatic colorectal metastases. Ann Royal Coll Surg Engl 78:27-30

Choi BI, Park JH, Kim BH et al (1989) Small hepatocellular carcinoma: detection with sonography, computed tomography (CT), angiography and lipiodol CT. Br J Radiol 62:897-903

Choi BI, Han JH, Song IS et al (1991) Intraoperative sonography of hepatocellular carcinoma: detection of lesions and validity in surgical resection. Gastrointest Radiol 16:329-333

Cosgrove DO, Bolondi L (1993) Malignant liver disease. In: Cosgrove D, Meire H, Dewbury K (eds) Abdominal and general ultrasound. Churchill Livingstone, Edinburgh, Scotland, pp 271-293

Dalla Palma L, Bertolotto M, Quaia E, Locatelli M (1999) Detection of liver metastases with pulse inversion harmonic imaging: preliminary results. Eur Radiol 9 [Suppl 3]:S382-S387

Del Frate C, Bazzocchi M, Mortele KJ et al (2002) Detection of liver metastases: comparison of gadobenate dimeglumine-enhanced and ferumoxides-enhanced MR imaging examinations. Radiology 225:766-772

Del Frate C, Zuiani C, LonderoV et al (2003) Comparing Levovist-enhanced pulse inversion harmonic imaging and ferumoxides-enhanced MR imaging of hepatic metastases. Am J Roentgenol 180:1339-1346

Forsberg F, Goldberg BB, Liu JB et al (1999) Tissue specific US contrast agent for evaluation of hepatic and splenic parenchyma. Radiology 209:125-132

Forsberg F, Liu JB, Chiou HJ et al (2000a) Comparison of fundamental and wideband harmonic contrast imaging of liver tumors. Ultrasonics 38:110-113

Forsberg F, Liu JB, Merton DA et al (2000b) Grayscale second harmonic imaging of acoustic emission signals improves detection of liver tumors in rabbits. J Ultrasound Med 19:557-563

Forsberg F, Piccoli CW, Liu JB et al (2002) Hepatic tumor detection: MR imaging and conventional US versus pulse-inversion harmonic US of NC100100 during its reticuloendothelial system-specific phase. Radiology 222:824-829

Harvey CJ, Albrecht T (2001) Ultrasound of focal liver lesions. Eur Radiol 11:1578-1593

Harvey CJ, Blomley MJ, Eckersley RJ et al (2000a) Pulse inversion mode imaging of liver specific microbubbles: improved detection of subcentimeter metastases. Lancet 355:807-808

Harvey CJ, Blomley MJ, Eckersley RJ et al (2000b) Hepatic malignancies: improved detection with pulse inversion US in late phase of enhancement with SH U 508 A – early experience. Radiology 216:903-908

Haspigel KD, Neidl KFW, Eichenberger AC et al (1995) Detection of liver metastases. Comparison of superparamagnetic iron oxide-enhanced and unenhanced MR imaging at 1.5 T with dynamic CT, intraoperative US and percutaneous US. Radiology 196:471-478

Hauff P, Fritsch T, Reinhardt M et al (1997) Delineation of experimental liver tumors in rabbits by a new ultrasound contrast agent and stimulated acoustic emission. Invest Radiol 32:94-99

Hope Simpson D, Chin CT, Burns PN (1999) Pulse inversion Doppler: a new method for detecting non-linear echoes from microbubble contrast agents. IEEE Trans Ultrason Ferroelectr Freq Contr 46:372-382

Kang BK, Lim JH, Kim SH et al (2003) Preoperative depiction of hepatocellular carcinoma: ferumoxides-enhanced MR imaging versus triple-phase helical CT. Radiology 226:79-85

Kindberg GM, Tolleshaug H, Roos N, Skotland T (2003) Hepatic clearance of Sonazoid perfluorobutane microbubbles by Kupffer cells does not reduce the ability of liver to phagocytose or degrade albumin microspheres. Cell Tissue Res 312:49-54

Laghi A, Iannaccone R, Rossi P et al (2003) Hepatocellular carcinoma: detection with triple-phase multi-detector row helical CT in patients with chronic hepatitis. Radiology 226:543-549

Lesavre A, Correas JM, Bridal L et al (2003) Efficacy of a specific ultrasound contrast agent in the detection of liver masses: quantitative evaluation and comparison to other US modalities (abstract). RSNA 2003

Lim AK, Patel N, Eckersley RJ et al (2004) Evidence of splenic-specific uptake of a microbubble contrast agent: a quantitative study in healthy volunteers. Radiology 231:785-788

Mosconi E, Quaia E, Bertolotto M et al (2003) Detection of liver metastases by pulse inversion harmonic imaging with Levovist in comparison to conventional ultrasound and with magnetic resonance imaging (MRI) with Gd-BOPTA as reference procedure. Eur Radiol 13 [Suppl 1]:365

Needleman L, Leen E, Kyriakkopoulou K et al (1998) NC100100: a new US contrast agent for fundamental and harmonic imaging of hepatic lesions (abstract). Radiology 209:189

Pauleit D, Textor J, Bachmann R (2002) Hepatocellular carcinoma: detection with gadolinium- and ferumoxides-enhanced MR imaging of the liver. Radiology 222:73-80

Quaia E, Bertolotto M, Ukmar M et al (2002a) Characterization of liver hemangiomas by pulse inversion harmonic imaging. Eur Radiol 12:537-544

Quaia E, Blomley MJK, Patel S et al (2002b) Initial observations on the effect of irradiation on the liver-specific uptake of Levovist. Eur J Radiol 41:192-199

Quaia E, Harvey CJ, Blomley MJK et al (2002c) Study of pulse inversion mode with the late phase of Levovist to detect hepatocellular carcinoma (HCC) in cirrhotic liver (abstract). ECR 2002

Quaia E, Bertolotto M, Forgács B et al (2003) Detection of liver metastases by pulse inversion harmonic imaging during Levovist late phase: comparison to conventional ultrasound and helical CT in 160 patients. Eur Radiol 13:475-483

Quaia E, Calliada F, Bertolotto M et al (2004) Characterization of focal liver lesions by contrast-specific US modes and a sulfur hexafluoride-filled microbubble contrast

agent: diagnostic performance and confidence. Radiology 232:420-430
Robinson PJA (2001) Imaging liver metastases: current limitations and future prospects. Br J Radiol 73:234-241
Seneterre E, Taourel P, Bouvier Y et al (1996) Detection of hepatic metastases: ferumoxides-enhanced MR imaging versus unenhanced MR imaging and CT during arterial portography. Radiology 200:785-792
Solbiati L, Cova L, Ierace T et al (2000) The importance of arterial phase imaging for wideband harmonic sonography for the characterization of focal liver lesions in liver cirrhosis using a second generation contrast agent (abstract). Radiology 217:305
Solbiati L, Tonolini M, Cova L, Goldberg N (2001) The role of contrast-enhanced ultrasound in the detection of focal liver lesions. Eur Radiol 11 [Suppl 3]:E15-E26
Soyer P, Lacheheb D, Levesque M (1992) False positive diagnosis based on CT portography: correlation with pathologic findings. Am J Roentgoenol 160:285-289
Takayasu K, Moriyama N, Muramatsu Y et al (1990) The diagnosis of small hepatocellular carcinoma: efficacy of various imaging procedures in 100 patients. Am J Roentgenol 155:49-54
Teefey SA, Hildeboldt CC, Dehdashti F et al (2003) Detection of primary hepatic malignancies in liver transplant candidates: prospective comparison of CT, MR imaging, US and PET. Radiology 226:533-542
Valls C, Lopez E, Guma A et al (1998) Helical CT versus CT arterial portography in the detection of hepatic metastases from colorectal carcinoma. Am J Roentgenol 170:1341-1347
Ward J, Naik KS, Guthrie JA et al (1999) Hepatic lesion detection: comparison of MR imaging after the administration of superparamagnetic iron oxide with dual phase CT by using alternative-free response receiver operating characteristic analysis. Radiology 210:459-466
Ward J, Cheng F, Guthrie JA et al (2000a) Hepatic lesion detection after superparamagnetic Iron oxide enhancement: comparison of five T2-weighted sequences at 1.0 T by using alternative-free response receiver operating characteristic analysis. Radiology 214:159-166
Ward J, Guthrie JA, Scott DJ et al (2000b) Hepatocellular carcinoma in the cirrhotic liver: double-contrast MR imaging for diagnosis. Radiology 216:154-162
Ward J, Guthrie JA, Wilson D et al (2003) Colorectal hepatic metastases: detection with SPIO-enhanced breath-hold MR imaging - comparison of optimized sequences. Radiology 228:709-718
Watanabe R, Matsumura M, Chen CJ et al (2003) Gray-scale liver enhancement with Sonazoid (NC100100), a novel ultrasound contrast agent; detection of hepatic tumors in a rabbit model. Biol Pharm Bull 26:1272-1277
Wernecke K, Rummeny E, Bongartz G et al (1991) Detection of hepatic masses in patients with carcinoma: comparative sensitivities of sonography, CT and MR imaging. AJR 157:731-739
Yamashita Y, Mitsuzaki K, Yi T et al (1996) Small hepatocellular carcinoma in patients with chronic liver damage: prospective comparison of detection with dynamic MR imaging and helical CT of the whole liver. Radiology 200:79-84